Supplementary Figure S1. Principle of suicidal conjugation assay and cassette orientation determination. A. During suicidal conjugation, either the top (ts) or the bottom strand (bs) of the *attC* site is delivered into the recipient cell, where it can be resynthesized, but cannot be replicated as pSW plasmid replication absolutely requires the Pir protein. **B.** However, the resistance marker can be maintained by integrating the plasmid carrying the *attC* into the plasmid containing an *attI* site, present in the recipient strain. The recombination can occur either with the delivered strand of the plasmid, or the resynthesized complementary strand. The frequency of recombination events was calculated as described in Supplementary Material S3. **C.** Depending whether the recombination occurred in the bottom or in the top strand, the orientation of cassette insertion varies, which was determined by performing PCR reactions on the resulting co-integrates, as described in Supplementary Material S5.

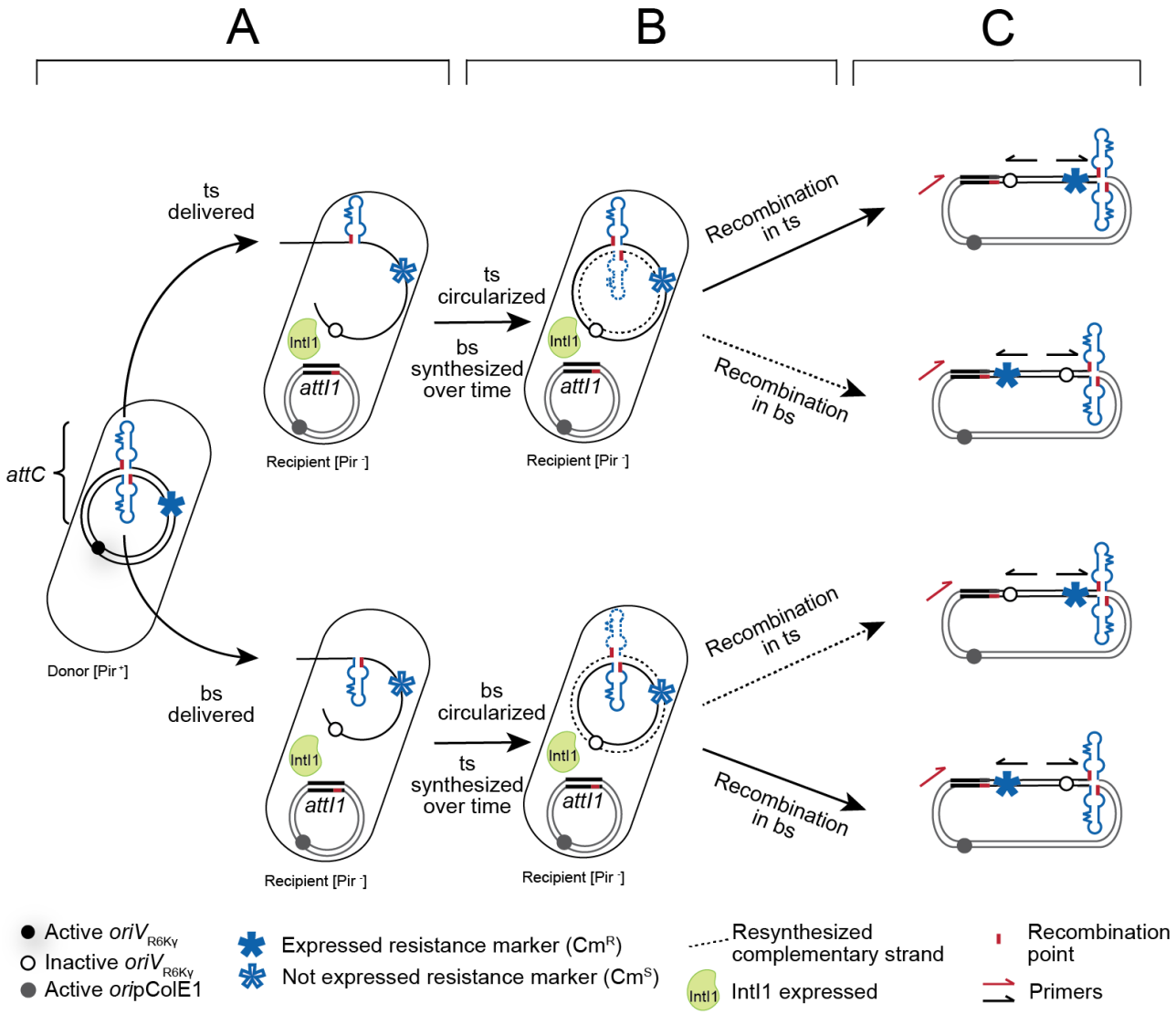

Supplementary Figure S2. The effect of R box sequence on strand selectivity. **A.** R box sequences of the tested mutants. **B-C.** The grey bars correspond to recombination frequencies of each strain: light green bars for recombination in the bottom strand; black bars for recombination in top strand. White cross-hatched bars correspond to the level of detection by PCR (see Supplementary Material S5), when recombination events of a particular strand were not observed. Error bars correspond to mean deviations. **B.** Recombination upon the delivery of the bottom strand (bs) of *attC* sites. **C.** Recombination upon the delivery of the top strand (ts) of *attC* sites.

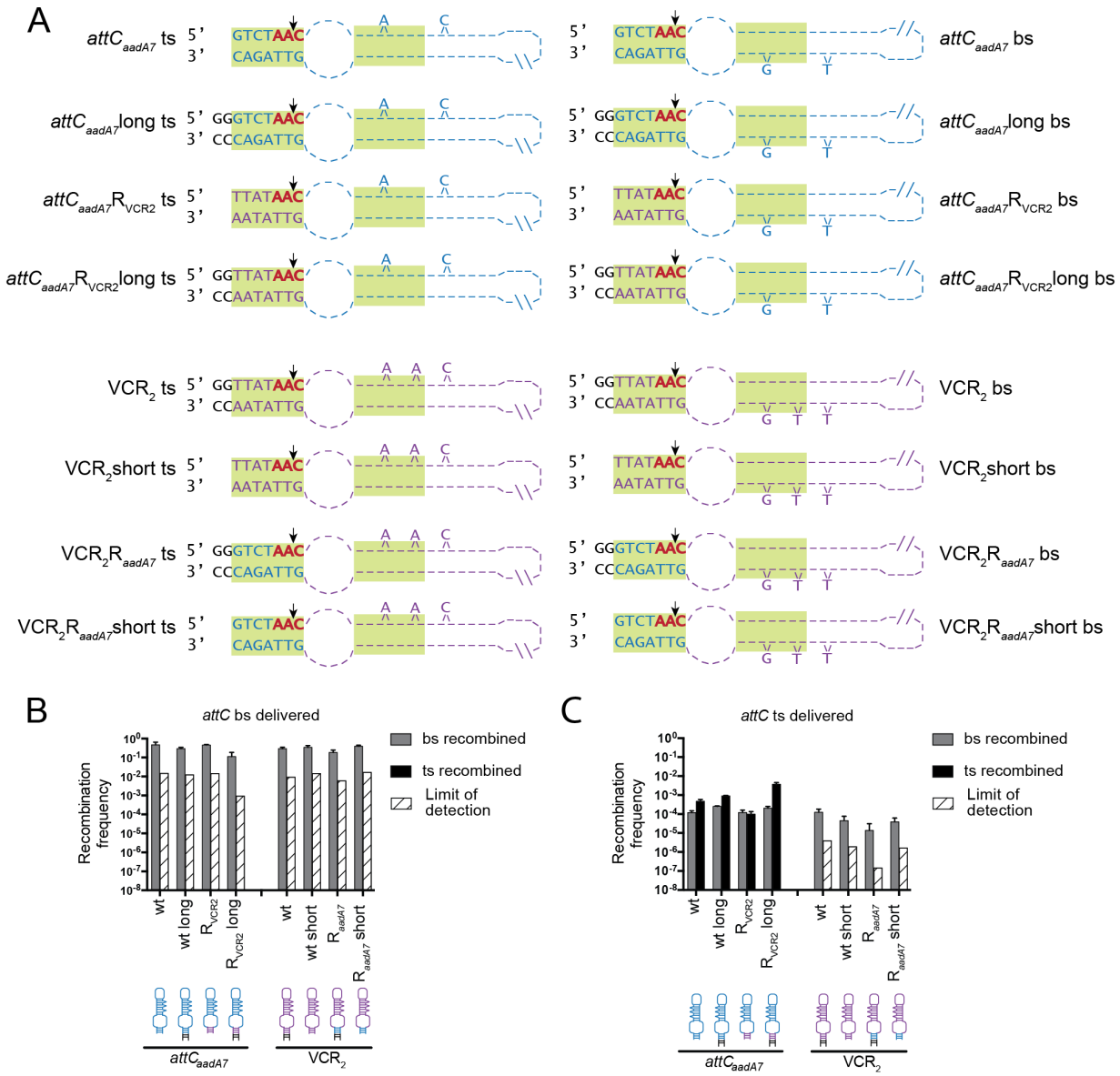

Supplementary Figure S3. Schematic representation of possible synapses formed during an *attI1*×*attC* recombination. A. Possible synapse formation between an *attI1* site and a wild-type *attC* site, for both its top (ts) and bottom (bs) strands. **B.** Possible synapse formation between an *attI1* site and an *attC* site with inverted EHBs, for both its top and bottom strands.

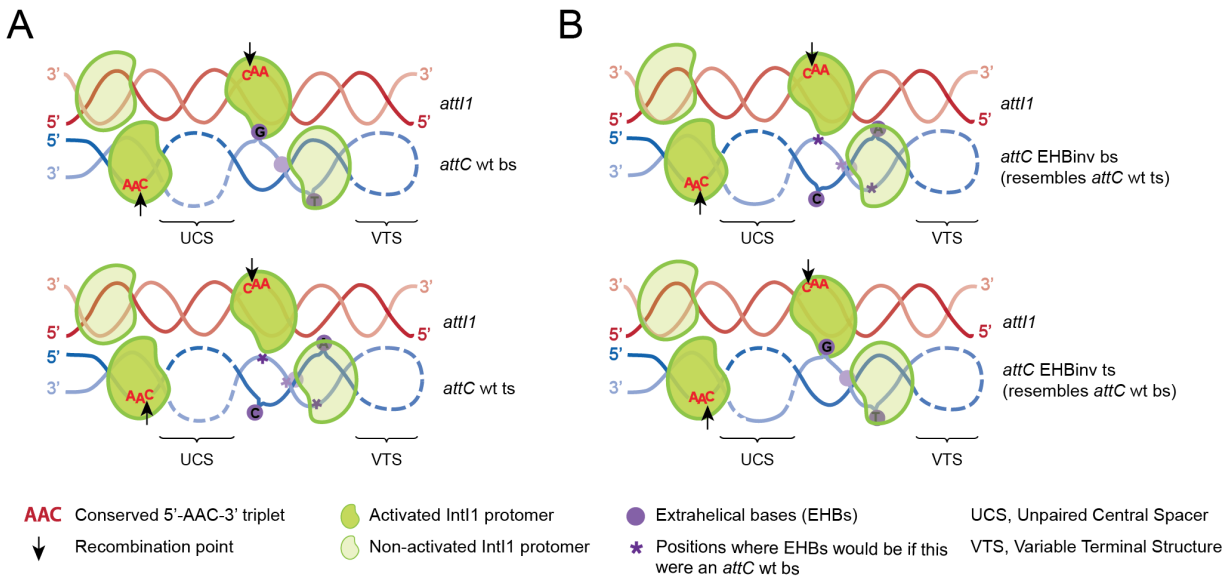

Supplementary Table S1. Oligonucleotides used in this study. Sequences are given in 5' → 3' direction.

A. DNA oligonucleotides used in the *in vivo* conjugation assay to generate the *attC* sites.

Primer name, number		Sequence
VCR_2	Fw1 #2980	GATCCGGTTATAACGCCCGCCTAAGGGGCTGACAACGCACTACCACTAAACTCAAACACAACAACAGCAACCACCGCGGCTCAAT
	Fw2 #2981	GGGACTGGAAACGCCACGCGTTGACAGTCCCTCTTGAGGCGTTTGTTATAACCG
	Rev1 #2982	AATTCGGTTATAACAAACGCCTCAAGAGGGACTGTCAACGCGTGGCGTTTCCAGTCCCATTGAGCCGCGGTGGTTGCTGTTGTTG
	Rev2 #2983	TGTTTGAGTTTAGTGGTAGTGCGTTGTCAGCCCCTTAGGCGGGCGTTATAACCG
$attC_{aadA7}$	Fw #3849	AATTCGTCTAACAATTCATTCAAGCCGACGCCGCTTCGCGGCGCGGCTTAATTCAAGCGTTAGACG
	Rev #3850	GATCCGTCTAACGCTTGAATTAAGCCGCGCCGCGAAGCGGCGTCGGCTTGAATGAATTGTTAGACG
$attC_{CATB3}$	Fw #3853	AATTCGTCTAACAATTCAATCAAGCCGATGCCGCTTCGCGGCACGGCTTATTTCAGGCGTTAGACG
	Rev #3854	GATCCGTCTAACGCCTGAAATAAGCCGTGCCGCGAAGCGGCATCGGCTTGATTGAATTGTTAGACG
$attC_{aadA5}$	Fw #3855	AATTCGCCTAACTCGGCGTTCAAGCGGACGGGCTGCGCCCGCCGCTCAACTATGCGTTAGGCG
	Rev #3856	GATCCGCCTAACGCATAGTTGAGCGGCGGGCGCAGCCCGTCCGCTTGAACGCCGAGTTAGGCG
$attC_{dfrB3}$	Fw #3857	AATTCGTTTAACTGGTCGCTCCAGCGGACGGCTTCGCCGCCCGCTGAGCTAGAGCGTTAAACG
	Rev #3858	GATCCGTTTAACGCTCTAGCTCAGCGGGCGGCGAAGCCGTCCGCTGGAGCGACCAGTTAAACG
VCR_2 ΔEHB	Fw1 #2980	GATCCGGTTATAACGCCCGCCTAAGGGGCTGACAACGCACTACCACTAAACTCAAACACAACAACAGCAACCACCGCGGCTCAA
	Fw2 #3859	TGGGACTGGAAACGCCACGCGTTGACAGCCCCTTAGGCGTTTGTTATAACCG
	Rev1 #3860	AATTCGGTTATAACAAACGCCTAAGGGGCTGTCAACGCGTGGCGTTTCCAGTCCCATTGAGCCGCGGTGGTTGCTGTTGTTG
	Rev2 #2983	TGTTTGAGTTTAGTGGTAGTGCGTTGTCAGCCCCTTAGGCGGGCGTTATAACCG
VCR_2 ΔG16	Fw1 #2980	GATCCGGTTATAACGCCCGCCTAAGGGGCTGACAACGCACTACCACTAAACTCAAACACAACAACAGCAACCACCGCGGCTCAA
	Fw2 #3861	TGGGACTGGAAACGCCACGCGTTGACAGTCCCTCTTAGGCGTTTGTTATAACCG
	Rev1 #3862	AATTCGGTTATAACAAACGCCTAAGAGGGACTGTCAACGCGTGGCGTTTCCAGTCCCATTGAGCCGCGGTGGTTGCTGTTGTTG
	Rev2 #2983	TGTTTGAGTTTAGTGGTAGTGCGTTGTCAGCCCCTTAGGCGGGCGTTATAACCG
VCR_2 ΔT20	Fw1 #2980	GATCCGGTTATAACGCCCGCCTAAGGGGCTGACAACGCACTACCACTAAACTCAAACACAACAACAGCAACCACCGCGGCTCAA
	Fw2 #3863	TGGGACTGGAAACGCCACGCGTTGACAGTCCCCTTGAGGCGTTTGTTATAACCG
	Rev1 #3864	AATTCGGTTATAACAAACGCCTCAAGGGGACTGTCAACGCGTGGCGTTTCCAGTCCCATTGAGCCGCGGTGGTTGCTGTTGTTG
	Rev2 #2983	TGTTTGAGTTTAGTGGTAGTGCGTTGTCAGCCCCTTAGGCGGGCGTTATAACCG
VCR_2 ΔT24	Fw1 #2980	GATCCGGTTATAACGCCCGCCTAAGGGGCTGACAACGCACTACCACTAAACTCAAACACAACAACAGCAACCACCGCGGCTCAA

	Fw2 #3865	TGGGACTGGAAACGCCACGCGTTGACAGCCCTCTTGAGGCGTTTGTTATAA CCG
	Rev1 #3866	AATTCGGTTATAACAAACGCCTCAAGAGGGCTGTCAACGCGTGGCGTTTCC AGTCCCATTGAGCCGCGGTGGTTGCTGTTGTTG
	Rev2 #2983	TGTTTGAGTTTAGTGGTAGTGCGTTGTCAGCCCCTTAGGCGGGCGTTATAA CCG
VCR_2 EHBinv	Fw1 #2984	GATCCGGTTATAACGCCCGCCTCAAGAGGGACTGACAACGCACTACCACTA AACTCAAACACAACAACAGCAACCACCGCGGCTC
	Fw2 #2985	AATGGGACTGGAAACGCCACGCGTTGACAGCCCCTTAGGCGTTTGTTATAA CCG
	Rev1 #2986	AATTCGGTTATAACAAACGCCTAAGGGGCTGTCAACGCGTGGCGTTTCCAG TCCCATTGAGCCGCGGTGGTTGCTGTTGTTGTGT
	Rev2 #2987	TTGAGTTTAGTGGTAGTGCGTTGTCAGTCCCTCTTGAGGCGGGCGTTATAA CCG
VCR_2 G16inv	Fw1 #2988	GATCCGGTTATAACGCCCGCCTCAAGGGGCTGACAACGCACTACCACTAAA CTCAAACACAACAACAGCAACCACCGCGGCTCAA
	Fw2 #2989	TGGGACTGGAAACGCCACGCGTTGACAGTCCCTCTTAGGCGTTTGTTATAA CCG
	Rev1 #2990	AATTCGGTTATAACAAACGCCTAAGAGGGACTGTCAACGCGTGGCGTTTCC AGTCCCATTGAGCCGCGGTGGTTGCTGTTGTTGT
	Rev2 #2991	GTTTGAGTTTAGTGGTAGTGCGTTGTCAGCCCCTTGAGGCGGGCGTTATAA CCG
VCR_2 T20inv T24inv	Fw1 #2992	GATCCGGTTATAACGCCCGCCTAAGAGGGACTGACAACGCACTACCACTAA ACTCAAACACAACAACAGCAACCACCGCGGCTCA
	Fw2 #2993	ATGGGACTGGAAACGCCACGCGTTGACAGCCCCTTGAGGCGTTTGTTATAA CCG
	Rev1 #2994	AATTCGGTTATAACAAACGCCTCAAGGGGCTGTCAACGCGTGGCGTTTCCA GTCCCATTGAGCCGCGGTGGTTGCTGTTGTTGTG
	Rev2 #2995	TTTGAGTTTAGTGGTAGTGCGTTGTCAGTCCCTCTTAGGCGGGCGTTATAA CCG
VCR_2 VTSinv	Fw1 #3867	GATCCGGTTATAACGCCCGCCTAAGGGGCTGACAACGCGTGGCGTTTCCA GTCCCATTGAGCCGCGGTGGTTGCTGTTGTTGTG
	Fw2 #3868	TTTGAGTTTAGTGGTAGTGCGTTGACAGTCCCTCTTGAGGCGTTTGTTATAA CCG
	Rev1 #3869	AATTCGGTTATAACAAACGCCTCAAGAGGGACTGTCAACGCACTACCACTA AACTCAAACACAACAACAGCAACCACCGCGGCT
	Rev2 #3870	CAATGGGACTGGAAACGCCACGCGTTGTCAGCCCCTTAGGCGGGCGTTAT AACCG
$attC_{oxa2}$ ΔEHB	Fw #2911	GATCCGCCCAACGTTGAAGTAACCGGCGCTGCGCGGTTTTATCGCGCAGC GCCGGTTACTGCCGGGTTGGGCGG
	Rev #2912	AATTCCGCCCAACCCGGCAGTAACCGGCGCTGCGCGATAAAACCGCGCAG CGCCGGTTACTTCAACGTTGGGCG
$attC_{oxa2}$ ΔG16	Fw #3871	GATCCGCCCAACGTTGAAGTAACCGGCGCTGCGCGGTTTTATCGCGCAGC GTCCGAGTTACTGCCGGGTTGGGCGG
	Rev #3872	AATTCCGCCCAACCCGGCAGTAACTCGGACGCTGCGCGATAAAACCGCGC AGCGCCGGTTACTTCAACGTTGGGCG
$attC_{oxa2}$ ΔA20	Fw #3873	GATCCGCCCAACGTTGAAGTAACCGGCGCTGCGCGGTTTTATCGCGCAGC GTCCGGTTGACTGCCGGGTTGGGCGG
	Rev #3874	AATTCCGCCCAACCCGGCAGTCAACCGGACGCTGCGCGATAAAACCGCGC AGCGCCGGTTACTTCAACGTTGGGCG
$attC_{oxa2}$ ΔT24	Fw #3875	GATCCGCCCAACGTTGAAGTAACCGGCGCTGCGCGGTTTTATCGCGCAGC GCCGAGTTGACTGCCGGGTTGGGCGG
	Rev #3876	AATTCCGCCCAACCCGGCAGTCAACTCGGCGCTGCGCGATAAAACCGCGC AGCGCCGGTTACTTCAACGTTGGGCG

attC$_{oxa2}$ G16inv	Fw #2905	GATCCGCCCAACGTTGAAGTCAACCGGCGCTGCGCGGTTTTATCGCGCAG CGTCCGAGTTACTGCCGGGTTGGGCGG
	Rev #2906	AATTCCGCCCAACCCGGCAGTAACTCGGACGCTGCGCGATAAAACCGCGC AGCGCCGGTTGACTTCAACGTTGGGCG
attC$_{oxa2}$ A20inv	Fw #2907	GATCCGCCCAACGTTGAAGTAACTCGGCGCTGCGCGGTTTTATCGCGCAG CGTCCGGTTGACTGCCGGGTTGGGCGG
	Rev #2908	AATTCCGCCCAACCCGGCAGTCAACCGGACGCTGCGCGATAAAACCGCGC AGCGCCGAGTTACTTCAACGTTGGGCG
attC$_{oxa2}$ T24inv	Fw #2909	GATCCGCCCAACGTTGAAGTAACCGGACGCTGCGCGGTTTTATCGCGCAG CGCCGAGTTGACTGCCGGGTTGGGCGG
	Rev #2910	AATTCCGCCCAACCCGGCAGTCAACTCGGCGCTGCGCGATAAAACCGCGC AGCGTCCGGTTACTTCAACGTTGGGCG
attC$_{oxa2}$ UCSinv	Fw #2913	GATCCGCCCAACCCGGCAGTAACCGGCGCTGCGCGGTTTTATCGCGCAGC GTCCGAGTTGACTTCAACGTTGGGCGG
	Rev #2914	AATTCCGCCCAACGTTGAAGTCAACTCGGACGCTGCGCGATAAAACCGCGC AGCGCCGGTTACTGCCGGGTTGGGCG
attC$_{oxa2}$ VTSinv	Fw #2926	GATCCGCCCAACGTTGAAGTAACCGGCGCTGCGCGATAAAACCGCGCAGC GTCCGAGTTGACTGCCGGGTTGGGCGG
	Rev #2927	AATTCCGCCCAACCCGGCAGTCAACTCGGACGCTGCGCGGTTTTATCGCG CAGCGCCGGTTACTTCAACGTTGGGCG
attC$_{aadA7}$ ΔEHB	Fw #3563	GATCCGTCTAACGCTTGAATTAAGCCGCGCCGCGAAGCGGCGCGGCTTAA TGAATTGTTAGACG
	Rev #3564	AATTCGTCTAACAATTCATTAAGCCGCGCCGCTTCGCGGCGCGGCTTAATT CAAGCGTTAGACG
attC$_{aadA7}$ ΔG16	Fw #3567	GATCCGTCTAACGCTTGAATTAAGCCGCGCCGCGAAGCGGCGTCGGCTTA ATGAATTGTTAGACG
	Rev #3568	AATTCGTCTAACAATTCATTAAGCCGACGCCGCTTCGCGGCGCGGCTTAAT TCAAGCGTTAGACG
attC$_{aadA7}$ ΔT23	Fw #3571	GATCCGTCTAACGCTTGAATTAAGCCGCGCCGCGAAGCGGCGCGGCTTGA ATGAATTGTTAGACG
	Rev #3572	AATTCGTCTAACAATTCATTCAAGCCGCGCCGCTTCGCGGCGCGGCTTAAT TCAAGCGTTAGACG
attC$_{aadA7}$ EHBinv	Fw #3565	GATCCGTCTAACGCTTGAATTCAAGCCGACGCCGCGAAGCGGCGCGGCTT AATGAATTGTTAGACG
	Rev #3566	AATTCGTCTAACAATTCATTAAGCCGCGCCGCTTCGCGGCGTCGGCTTGAA TTCAAGCGTTAGACG
attC$_{aadA7}$ G16inv	Fw #3569	GATCCGTCTAACGCTTGAATTCAAGCCGCGCCGCGAAGCGGCGTCGGCTT AATGAATTGTTAGACG
	Rev #3570	AATTCGTCTAACAATTCATTAAGCCGACGCCGCTTCGCGGCGCGGCTTGAA TTCAAGCGTTAGACG
attC$_{aadA7}$ T23inv	Fw #3573	GATCCGTCTAACGCTTGAATTAAGCCGACGCCGCGAAGCGGCGCGGCTTG AATGAATTGTTAGACG
	Rev #3574	AATTCGTCTAACAATTCATTCAAGCCGCGCCGCTTCGCGGCGTCGGCTTAA TTCAAGCGTTAGACG
attC$_{aadA7}$ T20supp	Fw #3559	AATTCGTCTAACAATTCATTCAAGACCGACGCCGCTTCGCGGCGCGGCTTA ATTCAAGCGTTAGACG
	Rev #3560	GATCCGTCTAACGCTTGAATTAAGCCGCGCCGCGAAGCGGCGTCGGTCTT GAATGAATTGTTAGACG
attC$_{aadA7}$ UCSinv	Fw #3575	GATCCGTCTAACAATTCATTAAGCCGCGCCGCGAAGCGGCGTCGGCTTGAA TTCAAGCGTTAGACG
	Rev #3576	AATTCGTCTAACGCTTGAATTCAAGCCGACGCCGCTTCGCGGCGCGGCTTA ATGAATTGTTAGACG
attC$_{aadA7}$ VTSinv	Fw #3581	GATCCGTCTAACGCTTGAATTAAGCCGCGCCGCTTCGCGGCGTCGGCTTG AATGAATTGTTAGACG

	Rev #3582	AATTCGTCTAACAATTCATTCAAGCCGACGCCGCGAAGCGGCGCGGCTTAATTCAAGCGTTAGACG
attC$_{aadA7}$ long	Fw #4169	AATTCGGGTCTAACAATTCATTCAAGCCGACGCCGCTTCGCGGCGCGGCTTAATTCAAGCGTTAGACCCG
	Rev #4170	GATCCGGGTCTAACGCTTGAATTAAGCCGCGCCGCGAAGCGGCGTCGGCTTGAATGAATTGTTAGACCCG
attC$_{aadA7}$ R$_{VCR2}$	Fw #3929	AATTCTTATAACAATTCATTCAAGCCGACGCCGCTTCGCGGCGCGGCTTAATTCAAGCGTTATAAG
	Rev #3930	GATCCTTATAACGCTTGAATTAAGCCGCGCCGCGAAGCGGCGTCGGCTTGAATGAATTGTTATAAG
attC$_{aadA7}$ R$_{VCR2}$ long	Fw #3381	GATCCGGTTATAACGCTTGAATTAAGCCGCGCCGCGAAGCGGCGTCGGCTTGAATGAATTGTTATAACCG
	Rev #3382	AATTCGGTTATAACAATTCATTCAAGCCGACGCCGCTTCGCGGCGCGGCTTAATTCAAGCGTTATAACCG
VCR$_2$ short	Fw1 #4165	AATTCTTATAACAAACGCCTCAAGAGGGACTGTCAACGCGTGGCGTTTCCAGTCCCATTGAGCCGCGGTGGTTGCTGTTGTTG
	Fw2 #4166	TGTTTGAGTTTAGTGGTAGTGCGTTGTCAGCCCCTTAGGCGGGCGTTATAAG
	Rev1 #4167	GATCCTTATAACGCCCGCCTAAGGGGCTGACAACGCACTACCACTAAACTCAAACACAACAACAGCAACCACCGCGGCTCAAT
	Rev2 #4168	GGGACTGGAAACGCCACGCGTTGACAGTCCCTCTTGAGGCGTTTGTTATAAG
VCR$_2$ R$_{aadA7}$	Fw1 #3939	AATTCGGGTCTAACAAACGCCTCAAGAGGGACTGTCAACGCGTGGCGTTTCCAGTCCCATTGAGCCGCGGTGGTTGCTGTTGTTG
	Fw2 #3940	TGTTTGAGTTTAGTGGTAGTGCGTTGTCAGCCCCTTAGGCGGGCGTTAGACCCG
	Rev1 #3941	GATCCGGGTCTAACGCCCGCCTAAGGGGCTGACAACGCACTACCACTAAACTCAAACACAACAACAGCAACCACCGCGGCTCAAT
	Rev2 #3942	GGGACTGGAAACGCCACGCGTTGACAGTCCCTCTTGAGGCGTTTGTTAGACCCG
VCR$_2$ R$_{aadA7}$ short	Fw1 #4171	AATTCGTCTAACAAACGCCTCAAGAGGGACTGTCAACGCGTGGCGTTTCCAGTCCCATTGAGCCGCGGTGGTTGCTGTTGTTG
	Fw2 #4172	TGTTTGAGTTTAGTGGTAGTGCGTTGTCAGCCCCTTAGGCGGGCGTTAGACG
	Rev1 #4173	GATCCGTCTAACGCCCGCCTAAGGGGCTGACAACGCACTACCACTAAACTCAAACACAACAACAGCAACCACCGCGGCTCAAT
	Rev2 #4174	GGGACTGGAAACGCCACGCGTTGACAGTCCCTCTTGAGGCGTTTGTTAGACG

B. DNA oligonucleotides used to identify the orientation of cassette insertion

Primer name	Sequence
SWbegin	CCGTCACAGGTATTTATTCGGCG
SWend	CCTCACTAAAGGGAACAAAAGCTG
MFD	CGCCAGGGTTTTCCCAGTCAC

C. DNA oligonucleotides used in the Electrophoretic Mobility Shift Assays (EMSA)

Primer name	Sequence
oxa2_wt_bs_EMSA	GGATCCGCCCAACGTTGAAGTAACCGGCGCTGCGCGGTTTTATCGCGCAGCGTCCGAGTTGACTGCCGGGTTGGGCGGAATTC
oxa2_wt_ts_EMSA	GAATTCCGCCCAACCCGGCAGTCAACTCGGACGCTGCGCGATAAAACCGCGCAGCGCCGGTTACTTCAACGTTGGGCGGATCC
oxa2_EHBdel_bs_EMSA	GGATCCGCCCAACGTTGAAGTAACCGGCGCTGCGCGGTTTTATCGCGCAGCGCCGGTTACTGCCGGGTTGGGCGGAATTC

oxa2_EHBdel_ts_EMSA	GAATTCCGCCCAACCCGGCAGTAACCGGCGCTGCGCGATAAAACCGC GCAGCGCCGGTTACTTCAACGTTGGGCGGATCC
oxa2_EHBinv_bs_EMSA	GGATCCGCCCAACGTTGAAGTCAACTCGGACGCTGCGCGGTTTTATC GCGCAGCGCCGGTTACTGCCGGGTTGGGCGGAATTC
aadA7_wt_bs_EMSA	GGATCCGTCTAACGCTTGAATTAAGCCGCGCCGCGAAGCGGCGTCGG CTTGAATGAATTGTTAGACGAATTC
aadA7_wt_ts_EMSA	GAATTCGTCTAACAATTCATTCAAGCCGACGCCGCTTCGCGGCGCGGC TTAATTCAAGCGTTAGACGGATCC
aadA7_EHBinv_bs_EMSA	GGATCCGTCTAACGCTTGAATTCAAGCCGACGCCGCGAAGCGGCGCG GCTTAATGAATTGTTAGACGAATTC
aadA7_EHBinv_ts_EMSA	GAATTCGTCTAACAATTCATTAAGCCGCGCCGCTTCGCGGCGTCGGCT TGAATTCAAGCGTTAGACGGATCC

Supplementary Table S2. Plasmids used in this study.

BOT, bottom strand of the *attC* site is delivered upon the conjugation of the plasmid; TOP, top strand of the *attC* site is delivered upon the conjugation of the plasmid.

Plasmid number	Plasmid description	Plasmid properties and construction
p3938	pBAD::*intI1*	*ori*ColE1; [$Carb^R$] (1)
p929	pSU38Δ::*attI1*	*ori*p15A; [Km^R] (2)
p4116	pSW23T::$attC_{aadA7}$T23inv (BOT)	$oriV_{R6K\gamma}$, $oriT_{RP4}$;[Cm^R] (3)
p4117	pSW23T::$attC_{aadA7}$T23inv (TOP)	$oriV_{R6K\gamma}$, $oriT_{RP4}$;[Cm^R] (3)
pC510	pSW23T::VCR_2 (BOT)	Annealing of primers and cloning into p4116
pC514	pSW23T::VCR_2 (TOP)	Annealing of primers and cloning into p4117
pD060	pSW23T::$attC_{aadA7}$ (BOT)	Annealing of primers and cloning into p4116
pD059	pSW23T::$attC_{aadA7}$ (TOP)	Annealing of primers and cloning into p4117
pD823	pSW23T::$attC_{CATB3}$ (BOT)	Annealing of primers and cloning into p4116
pD824	pSW23T::$attC_{CATB3}$ (TOP)	Annealing of primers and cloning into p4117
pD044	pSW23T::$attC_{aadA5}$ (BOT)	Annealing of primers and cloning into p4116
pD043	pSW23T::$attC_{aadA5}$ (TOP)	Annealing of primers and cloning into p4117
pD046	pSW23T::$attC_{dfrB3}$ (BOT)	Annealing of primers and cloning into p4116
pD045	pSW23T::$attC_{dfrB3}$ (TOP)	Annealing of primers and cloning into p4117
p3652	pSW23T::$attC_{ereA2}$ (BOT)	Constructed in a previous study (3)
p4393	pSW23T::$attC_{ereA2}$ (TOP)	Constructed in a previous study (3)
pC302	pSW23T::$attC_{oxa2}$ (BOT)	Constructed in a previous study (3)
pC303	pSW23T::$attC_{oxa2}$ (TOP)	Constructed in a previous study (3)
pD056	pSW23T::VCR_2ΔEHB (BOT)	Annealing of primers and cloning into p4116

pD055	pSW23T::VCR$_2$ΔEHB (TOP)	Annealing of primers and cloning into p4117
pD050	pSW23T::VCR$_2$ΔG16 (BOT)	Annealing of primers and cloning into p4116
pD049	pSW23T::VCR$_2$ΔG16 (TOP)	Annealing of primers and cloning into p4117
pD052	pSW23T::VCR$_2$ΔT20 (BOT)	Annealing of primers and cloning into p4116
pD051	pSW23T::VCR$_2$ΔT20 (TOP)	Annealing of primers and cloning into p4117
pD054	pSW23T::VCR$_2$ΔT24 (BOT)	Annealing of primers and cloning into p4116
pD053	pSW23T::VCR$_2$ΔT24 (TOP)	Annealing of primers and cloning into p4117
pC511	pSW23T::VCR$_2$EHBinv (BOT)	Annealing of primers and cloning into p4116
pC515	pSW23T::VCR$_2$EHBinv (TOP)	Annealing of primers and cloning into p4117
pC512	pSW23T::VCR$_2$G16inv (BOT)	Annealing of primers and cloning into p4116
pC516	pSW23T::VCR$_2$G16inv (TOP)	Annealing of primers and cloning into p4117
p4160	pSW23T::VCR$_2$T20inv (BOT)	Constructed in a previous study (3)
p4161	pSW23T::VCR$_2$T20inv (TOP)	Constructed in a previous study (3)
p4132	pSW23T::VCR$_2$T24inv (BOT)	Constructed in a previous study (3)
p4177	pSW23T::VCR$_2$T24inv (TOP)	Constructed in a previous study (3)
pC513	pSW23T::VCR$_2$T20invT24inv (BOT)	Annealing of primers and cloning into p4116
pC517	pSW23T::VCR$_2$T20invT24inv (TOP)	Annealing of primers and cloning into p4117
p3427	pSW23T::VCR$_2$UCSinv (BOT)	Constructed in a previous study (3)
pD899	pSW23T::VCR$_2$UCSinv (TOP)	Constructed in a previous study (3)
pD058	pSW23T::VCR$_2$VTSinv (BOT)	Annealing of primers and cloning into p4116
pD057	pSW23T::VCR$_2$VTSinv (TOP)	Annealing of primers and cloning into p4117
pC650	pSW23T::*attC*$_{oxa2}$ΔEHB (BOT)	Annealing of primers and cloning into p4116
pC395	pSW23T::*attC*$_{oxa2}$ΔEHB (TOP)	Annealing of primers and cloning into p4117
pC651	pSW23T::*attC*$_{oxa2}$ΔG16 (BOT)	Annealing of primers and cloning into p4116
pC652	pSW23T::*attC*$_{oxa2}$ΔG16 (TOP)	Annealing of primers and cloning into p4117
pC653	pSW23T::*attC*$_{oxa2}$ΔA20 (BOT)	Annealing of primers and cloning into p4116
pC654	pSW23T::*attC*$_{oxa2}$ΔA20 (TOP)	Annealing of primers and cloning into p4117
pC655	pSW23T::*attC*$_{oxa2}$ΔT24 (BOT)	Annealing of primers and cloning into p4116
pC656	pSW23T::*attC*$_{oxa2}$ΔT24 (TOP)	Annealing of primers and cloning into p4117
pD900	pSW23T::*attC*$_{oxa2}$EHBinv (BOT)	Constructed in a previous study (3)
p4439	pSW23T::*attC*$_{oxa2}$EHBinv (TOP)	Constructed in a previous study (3)

pC293	pSW23T::*attC*$_{oxa2}$G16inv (BOT)	Annealing of primers and cloning into p4116
pC392	pSW23T::*attC*$_{oxa2}$G16inv (TOP)	Annealing of primers and cloning into p4117
pC294	pSW23T::*attC*$_{oxa2}$A20inv (BOT)	Annealing of primers and cloning into p4116
pC393	pSW23T::*attC*$_{oxa2}$A20inv (TOP)	Annealing of primers and cloning into p4117
pC295	pSW23T::*attC*$_{oxa2}$T24inv (BOT)	Annealing of primers and cloning into p4116
pC394	pSW23T::*attC*$_{oxa2}$T24inv (TOP)	Annealing of primers and cloning into p4117
pC297	pSW23T::*attC*$_{oxa2}$UCSinv (BOT)	Annealing of primers and cloning into p4116
pC396	pSW23T::*attC*$_{oxa2}$UCSinv (TOP)	Annealing of primers and cloning into p4117
pC298	pSW23T::*attC*$_{oxa2}$VTSinv (BOT)	Annealing of primers and cloning into p4116
pC397	pSW23T::*attC*$_{oxa2}$VTSinv (TOP)	Annealing of primers and cloning into p4117
pD807	pSW23T::*attC*$_{aadA7}$ΔEHB (BOT)	Annealing of primers and cloning into p4116
pD808	pSW23T::*attC*$_{aadA7}$ΔEHB (TOP)	Annealing of primers and cloning into p4117
pD803	pSW23T::*attC*$_{aadA7}$ΔG16(BOT)	Annealing of primers and cloning into p4116
pD804	pSW23T::*attC*$_{aadA7}$ΔG16(TOP)	Annealing of primers and cloning into p4117
pD805	pSW23T::*attC*$_{aadA7}$ΔT23(BOT)	Annealing of primers and cloning into p4116
pD806	pSW23T::*attC*$_{aadA7}$ΔT23(TOP)	Annealing of primers and cloning into p4117
pD813	pSW23T::*attC*$_{aadA7}$EHBinv (BOT)	Annealing of primers and cloning into p4116
pD814	pSW23T::*attC*$_{aadA7}$EHBinv (TOP)	Annealing of primers and cloning into p4117
pD809	pSW23T::*attC*$_{aadA7}$G16inv (BOT)	Annealing of primers and cloning into p4116
pD810	pSW23T::*attC*$_{aadA7}$G16inv (TOP)	Annealing of primers and cloning into p4117
pD811	pSW23T::*attC*$_{aadA7}$T23inv (BOT)	Annealing of primers and cloning into p4116
pD812	pSW23T::*attC*$_{aadA7}$T23inv (TOP)	Annealing of primers and cloning into p4117
pD819	pSW23T::*attC*$_{aadA7}$T20supp (BOT)	Annealing of primers and cloning into p4116
pD820	pSW23T::*attC*$_{aadA7}$T20supp (TOP)	Annealing of primers and cloning into p4117
pD815	pSW23T::*attC*$_{aadA7}$UCSinv (BOT)	Annealing of primers and cloning into p4116
pD816	pSW23T::*attC*$_{aadA7}$UCSinv (TOP)	Annealing of primers and cloning into p4117
pD817	pSW23T::*attC*$_{aadA7}$VTSinv (BOT)	Annealing of primers and cloning into p4116
pD818	pSW23T::*attC*$_{aadA7}$VTSinv (TOP)	Annealing of primers and cloning into p4117
pE932	pSW23T::*attC*$_{aadA7}$long (BOT)	Annealing of primers and cloning into p4116
pE931	pSW23T::*attC*$_{aadA7}$long (TOP)	Annealing of primers and cloning into p4117
pE612	pSW23T::*attC*$_{aadA7}$R$_{VCR2}$ (BOT)	Annealing of primers and cloning into p4116

pE613	pSW23T::*attC*$_{aadA7}$R$_{VCR2}$ (TOP)	Annealing of primers and cloning into p4117
pC299	pSW23T::*attC*$_{aadA7}$R$_{VCR2}$long (BOT)	Annealing of primers and cloning into p4116
pC518	pSW23T::*attC*$_{aadA7}$R$_{VCR2}$long (TOP)	Annealing of primers and cloning into p4117
pE930	pSW23T::VCR$_2$short (BOT)	Annealing of primers and cloning into p4116
pE929	pSW23T::VCR$_2$short (TOP)	Annealing of primers and cloning into p4117
pE622	pSW23T::VCR$_2$R$_{aadA7}$ (BOT)	Annealing of primers and cloning into p4116
pE623	pSW23T::VCR$_2$R$_{aadA7}$ (TOP)	Annealing of primers and cloning into p4117
pE934	pSW23T::VCR$_2$R$_{aadA7}$short (BOT)	Annealing of primers and cloning into p4116
pE933	pSW23T::VCR$_2$R$_{aadA7}$short (TOP)	Annealing of primers and cloning into p4117

Supplementary Material S1. Bacterial strains and media

Bacterial strains used in this study are DH5α, Π1, and β2163 (4). Plasmids are described in the Supporting Table S2. *Escherichia coli* strains were grown in Luria-Bertani (LB) broth at 37°C. Antibiotics were used at the following concentrations: chloramphenicol (Cm), 25 µg/ml; kanamycin (Km), 25 µg/ml; carbenicillin (Carb), 100 µg/ml. Thymidine (Thy) and diaminopimelic acid (DAP) were supplemented when necessary to a final concentration of 0.3 mM. To induce the P_{BAD} promoter, arabinose (Ara) was added to a final concentration of 2mg/ml; to repress it, glucose (Glc) was added to a final concentration of 10mg/ml.

Supplementary Material S2. *attC* site folding.

In this work, by *attC* site sequence we mean the sequence between R' and R'' (including them), the variable 4bp of the R' being complementary to their counterparts in the R''. In fact, this fully complementary sequence corresponds to a cassette-associated *attC* site: upon integration into an *attI*, the part of the R' of the *attC* site that is localized in the 5' moiety relative to the recombination point (Fig.1C, to the left of the arrow in the ss-*attC* bs and ss-*attC* ts) becomes cleaved from the rest of the site, and the R box of the integrated *attC* site inherits this 5' moiety from the *attI* sequence (Fig.1C, to the right of the arrow in the ds-*attI1*). Upon excision, the complementary sequence is once again reconstituted. For the VCR_2, we added two extra bases on each extremity of the site, to obtain an exact copy of the one that was studied before (3, 5) (see Figure 2B).

The structures of folded top and bottom strands of *attC* sites are represented in Fig.3B. All structures were obtained by RNAfold program from the ViennaRNA2 package (6) with the set of DNA-folding parameters derived from Mathews *et al.* (2004) (7), using the `-p` option to compute the partition function and plot the predicted structure, as well as the `-C` option for adding a constraint to pair the R' and R'', and L' and L'' sequences, respectively. We have used this last option to represent the structures that are most likely to be recombinogenic, instead of alternative favourable, but non-recombinogenic structures that could be formed (8). Indeed, integrase binding stabilizes *attC* sites and favorizes their recombination *in vitro* and *in vivo* (9), thus constraining the R and L boxes to pair, as seen in the crystal structure of VchIntIA bound to two *VCR2* sites (10). Even though in some cases the structure given by RNAfold does not comply with the imposed constraint (as in the case of the incompletely paired L box of $attC_{aadA7}$), it is likely that *in vivo*, the boxes will become fully paired upon integrase binding.

Supplementary Material S3. Suicidal conjugation assay.

This assay was previously developed (2) and implemented (3, 5) for the study of *attC* site recombination. It consists of delivering one strand of a plasmid, carrying either the top or the bottom strand of an *attC* site, into a recipient strain expressing IntI1 integrase and capable of performing an *attI1*×*attC* reaction (Fig.4). The donor strain β2163 requires DAP to grow in rich medium, and contains the RP4 conjugative transfer system and the *pir* gene on its chromosome. The latter allows the replication of a pSW23T plasmid with a *pir*-dependent origin of replication *oriV*R6Kγ(4), which carries an RP4 transfer origin, an *attC* site and a chloramphenicol resistance marker. Depending on the pSW23T-based vector used for cloning, the strand transferred by β2163 during conjugation carries either a bottom strand of the *attC* site (p4116 as vector) or a top strand (p4117 as vector). The recipient DH5α strain expresses the IntI1 integrase from a pBAD plasmid (p3938) and carries a pSU38Δ plasmid containing an *attI1* site (p929), but is unable to maintain the replication of the *pir*-dependent pSW23T plasmid that is transferred into the recipient by conjugation. The only way to maintain its replication and express the encoded chloramphenicol resistance marker is to insert pSW23T as a cassette into the pSU38Δ plasmid through *attI1*×*attC* recombination.

For this assay, the donor and the recipient strains were grown overnight with the corresponding antibiotics and other chemicals (Km, Cm and DAP for the donor; Km, Carb and Glc for the recipient), then diluted 1:100 with the corresponding antibiotics and other chemicals (Km and DAP for the donor; Km and Ara for the recipient) and grown until the OD_{600}=0.4 to 0.5. Then, 1ml of donor and 1ml of recipient cultures were mixed, centrifuged, and the pellet was spread on a 0.45µm filter placed on a LB-agarose media supplemented with DAP and Ara, for an overnight conjugation. The filter was then resuspended in 5ml LB media, after which serial 1:10 dilutions were made by the "easySpiral Dilute®" automatic serial diluter and plater. 50µl of the initial solution and of the 10^{-2} dilution were exponentially plated on LB-

agarose media supplemented with Cm; 50µl of the 10^{-4} dilution was exponentially plated on LB-agarose media supplemented with Km. This patented and approved exponential plating method allows the user to plate several dilutions on a single plate. It is compatible with the "Scan® 300" automatic colony counter, which was used to count the number of colony-forming units (CFU) on each plate and determine the initial bacterial concentrations. The recombination frequency was calculated as the ratio of recombinant CFUs [Cm^R] to the total number of recipient CFUs [Km^R]. For each strain, the overall recombination frequency is a mean of 3 independent experiments, and error bars represent the mean deviation (Fig.5 and 7).

Supplementary Material S4. Test of conjugation efficiency.

To prove that the differences in recombination frequencies were not due to differences in conjugation, we verified that for all strains, their conjugation frequencies were comparable, and indeed they were between 8×10^{-2} and 4×10^{-1}. It was performed by a similar protocol as described above, but using a Π1 strain as recipient, which is *pir*$^+$ and allows pSW23T plasmid replication (this strain has to be supplemented with Thymine). Conjugation frequencies were calculated as the ratio of [Cm^R] colonies to the total number of recipient colonies.

Supplementary Material S5. Determination of cassette insertion orientation

The recombination frequencies in the bottom and top strands, as well as the corresponding mean deviations were deduced by determining the orientation of cassette insertion for at least 20 independent clones for each strain (Fig.2C and D and Fig.3). For each clone, the orientation of cassette insertion was determined by performing two PCR reactions, as previously described(3) (for primer sequences, see the Supplementary Table S1B): the first reaction with SW23begin/MFD primers produced a product only when the recombination took place in the delivered *attC* strand (in the bottom strand, 530bp; in the top, 520bp); the second reaction with SW23end/MFD primers produced a product only when the recombination took place in the resynthesized *attC* strand (in the top strand when the bottom strand is delivered, 240bp; in the bottom strand when the top strand is delivered, 210bp). When recombination events were detected in both bottom and top strands, the values of grey and black bars were calculated by multiplying the overall recombination frequency of this mutant by the proportion of recombination events happening correspondingly in the bottom and in the top strands, as determined by the PCR reactions. When recombination events were detected only in one strand, the corresponding recombination frequency was attributed entirely to recombination in that strand, and a limit of detection was calculated for the other strand. This limit of detection is due to the limited number of CFUs that could be tested for each mutant, and corresponds to minimal frequency of recombination that could possibly be detected by this method. It is calculated as the overall recombination frequency divided by the number od CFUs tested.

1. Demarre,G., Frumerie,C., Gopaul,D.N. and Mazel,D. (2007) Identification of key structural determinants of the IntI1 integron integrase that influence attC x attI1 recombination efficiency. *Nucleic Acids Research*, **35**, 6475–6489.

2. Biskri,L., Bouvier,M., Guerout,A.-M., Boisnard,S. and Mazel,D. (2005) Comparative study of class 1 integron and Vibrio cholerae superintegron integrase activities. *Journal of Bacteriology*, **187**, 1740–1750.

3. Bouvier,M., Ducos-Galand,M., Loot,C., Bikard,D. and Mazel,D. (2009) Structural features of single-stranded integron cassette attC sites and their role in strand selection. *PLoS Genet*, **5**, e1000632.

4. Demarre,G., Guerout,A.-M., Matsumoto-Mashimo,C., Rowe-Magnus,D.A., Marlière,P. and Mazel,D. (2005) A new family of mobilizable suicide plasmids based on broad host range R388 plasmid (IncW) and RP4 plasmid (IncPalpha) conjugative machineries and their cognate Escherichia coli host strains. *Research in Microbiology*, **156**, 245–255.

5. Bouvier,M., Demarre,G. and Mazel,D. (2005) Integron cassette insertion: a recombination process involving a folded single strand substrate. *EMBO J.*, **24**, 4356–4367.

6. Lorenz,R., Bernhart,S.H., Höner Zu Siederdissen,C., Tafer,H., Flamm,C., Stadler,P.F. and Hofacker,I.L. (2011) ViennaRNA Package 2.0. *Algorithms Mol Biol*, **6**, 26.

7. Mathews,D.H., Disney,M.D., Childs,J.L., Schroeder,S.J., Zuker,M. and Turner,D.H. (2004) Incorporating chemical modification constraints into a dynamic programming algorithm for prediction of RNA secondary structure. *Proc. Natl. Acad. Sci. U.S.A.*, **101**, 7287–7292.

8. Loot,C., Bikard,D., Rachlin,A. and Mazel,D. (2010) Cellular pathways controlling integron cassette site folding. *EMBO J.*, **29**, 2623–2634.

9. Loot,C., Parissi,V., Escudero,J.A., Amarir-Bouhram,J., Bikard,D. and Mazel,D. (2014) The Integron Integrase Efficiently Prevents the Melting Effect of Escherichia coli Single-Stranded DNA-Binding Protein on Folded attC Sites. *Journal of Bacteriology*, **196**, 762–771.

10. MacDonald,D., Demarre,G., Bouvier,M., Mazel,D. and Gopaul,D.N. (2006) Structural basis for broad DNA-specificity in integron recombination. *Nature*, **440**, 1157–1162.